Easy-to-Operate and Low-Temperature Synthesis of Gram-Scale Nitrogen-Doped Graphene and Its Application as Cathode Catalyst in Microbial Fuel Cells

Leiyu Feng,[†] Yinguang Chen,[†,*] and Lang Chen[‡]

[†]State Key Laboratory of Pollution Control and Resources Reuse, School of Environmental Science and Engineering, Tongji University, Shanghai 200092, People's Republic of China and, [‡]School of Physics, Huazhong University of Science and Technology, Wuhan 430074, People's Republic of China

ABSTRACT

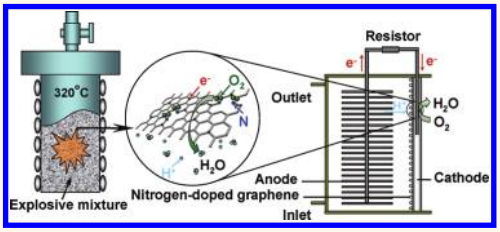

Nitrogen-doped graphene (NG), with unique electronic properties, is showing great promise for a wide range of practical applications. However, the reported approaches for NG synthesis are usually complex, require high temperatures, produce lower atomic ratios of nitrogen to carbon (N/C), and do not deliver products in a reasonably large quantity. Here we report an easy-to-operate and low-temperature method to synthesize NG in gram-scale quantities with a denotation process. High-resolution transmission electron microscopy, Raman spectroscopy, and X-ray diffraction characterization suggested that the synthesized NG films were uniformly multilayered and had a high crystalline quality. In the graphene sheets the existence of nitrogen substitution with an atomic ratio of N/C 12.5%, which was greater than those reported in the literature, was confirmed by X-ray photoelectron spectroscopic analysis. In the neutral phosphate buffer solution, the synthesized NG was demonstrated to act as a metal-free electrode with excellent electrocatalytic activity and long-term operation stability for oxygen reduction *via* a combination of two-electron and four-electron pathways. When the NG was applied as the cathode catalyst of microbial fuel cells (MFCs), the obtained maximum power density was comparable to that of conventional platinum catalyst. More importantly, MFCs with NG produced power more stably and less expensively than those with Pt catalyst, indicating that the synthesized NG might be used as a good alternative to Pt catalyst in MFCs with a long run.

KEYWORDS: graphene · nitrogen doping · low-temperature synthesis · denotation process · microbial fuel cells

Graphene, as an emerging two-dimensional (2-D) structure of free-standing carbon atoms packed into a dense honeycomb crystal structure, has draw wide attention due to its great promise for applications in many fields, such as supercapacitors,[1] sensors,[2] and energy storage.[3] Recently, doping graphene with nitrogen atoms was demonstrated to be an effective method to intrinsically tailor its electronic properties,[4−7] which created novel nanomaterials and expanded potential applications. For example, nitrogen-doped graphene (NG) has been found to have a high electrocatalytic activity for oxygen reduction reaction (ORR) in the alkaline solution, with a great potential as metal-free catalyst in fuel cells.[7] However, until now the reported methods for NG synthesis are usually complex, require high temperatures, produce lower atomic ratios of nitrogen to carbon (N/C) in products, and do not deliver a reasonably large quantity of products, which is very important for real-world applications.[7−12] Moreover, most of graphene doped with nitrogen was prepared by using metal catalysts, making it difficult to distinguish whether the catalytic activity of NG is caused by its unique electronic properties or by some metal residue.[13] The exploration of an easy-to-operate, low-temperature, and catalyst-free method for large-scale synthesis of NG with a higher atomic ratio of N/C is therefore highly desirable.

In recent years, microbial fuel cells (MFCs), a new method to generate current from organic and inorganic matter, have also attracted wide-ranging interest.[14,15] Similarly to the classical fuel cells, MFCs are basically composed of an anode, on which the fuel is oxidized by microorganisms, and a cathode that consumes the electrons generally by an oxidant. Various oxidants have been used as electron acceptors at the cathode of MFCs, whereas the most sustainable electron acceptor is oxygen due to its easy availability in the environment with the capacity to give a high power output.[16,17] Promising applications of MFCs include energy recovery from

* Address corresponding to yinguangchen@yahoo.com.

Received for review July 31, 2011 and accepted October 27, 2011.

Published online October 27, 2011
10.1021/nn202906f

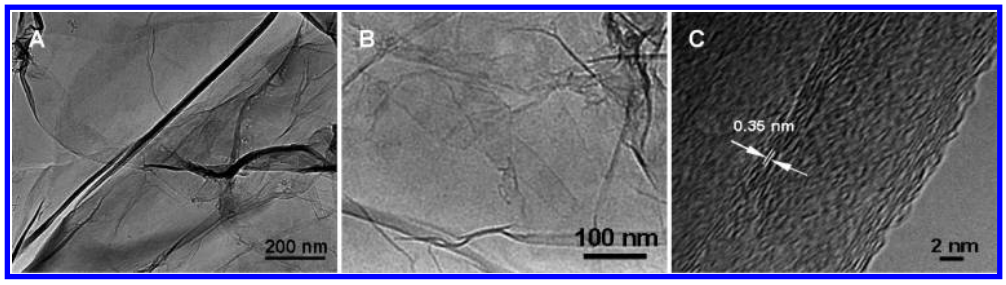

Figure 1. TEM analyses of the synthesized NG films. Low-resolution TEM images of the NG films (A, B). The graphene film is crumpled with many ripples. HRTEM image of the NG films showing edges of the N-graphene film regions consisting of *ca.* 4−8 graphene layers (C).

wastewater,[18] marine sediment,[19] and biomass.[20] However, many challenges, such as the technical issues associated with the performance and stability, must be overcome before MFCs are practical for renewable energy production. Among those challenges, the high cost of constructing MFCs is considered to be the most formidable and has driven much of the applied and fundamental MFC research. According to the cost analysis, the cathode catalysts are by far the most expensive constituents, accounting for more than half of the MFC cost, as catalysts at the cathode are usually based on platinum (Pt) or platinum alloys, although MFCs also use several other high-priced components. The price of Pt at present is as high as about $1800 per troy ounce, and an increase in the demand for fuel cell systems is bound to drive up the already high price of Pt. Thus, the development of efficient, stable, and less expensive alternatives to Pt and Pt-based catalysts represents an important research field in MFCs.

In this paper, we report a facile method for large-scale preparation of NG using a detonation technique with cyanuric chloride and trinitrophenol as reactants, which are low cost and easily accessible. This method features a much easier operation and lower synthesis temperature than previously reported. Moreover, no metal catalysts were used during the preparation of graphene material. The electrocatalytic activity of synthesized NG for ORR in the neutral pH medium, which as far as we are aware is still unknown, was also examined. Finally, the synthesized NG was applied as the cathode catalyst in MFCs, and its performance was compared with the commonly used Pt catalyst.

RESULTS AND DISCUSSION

Recently, a number of approaches, such as chemical vapor deposition (CVD),[7−9] arc-discharge,[10] and post-treatments,[6,11] have been proposed to synthesize NG. All these documented methods, however, were complex and operated at high temperatures (800−1100 °C). Herein, we used a detonation process to synthesize N-graphene films. In a typical procedure, the detonation reaction of cyanuric chloride (2 g) and trinitrophenol (3 g) was carried out at 320 °C with a momentary pressure of 60 MPa and an equilibrium pressure of 30 MPa in a 20 mL stainless steel autoclave (Figure S1 in the Supporting Information). After the autoclave was cooled to room temperature, the gaseous products were discharged and black solid NG was collected. The black solid product was then washed sequentially with water and ethanol, followed by drying at 105 °C for 1 h. The final yield of NG was approximately 0.1 g per 1 g of cyanuric chloride, typically yielding ∼0.2 g per batch. It can be seen that our method for NG synthesis was easier to operate and at a much lower temperature and allowed a large-scale yield. Also, the metal catalysts usually used for the growth of graphene material did not appear throughout the preparation of NG. The synthesized NG was therefore completely metal-free, which was evidenced by X-ray photoelectron spectroscopic (XPS) analysis in the following text.

Figure 1A−C show the morphologies and structures of the synthesized NG characterized with TEM. As seen in Figure 1A and B, the film had a morphology resembling large crumpled paper, indicating that the NG was flexible. The rumpling of the graphene layer might come from the growth process and could also be observed in the graphene produced in the absence of nitrogen sources.[21,22] The high-resolution TEM image (HRTEM, Figure 1C) further revealed the thickness of the graphene films and the detailed crystalline structure of the NG. As observed from the HRTEM image, the NG, produced here, was graphene with 4−8 graphitic layers and the interlayer distance was about 0.35 nm, which was in line with that of graphite.

Raman spectroscopy is a powerful tool for identifying the crystalline quality of carbon materials. Figure 2 shows the Raman spectrum of synthesized NG. A high density of the D band (1328 cm^{-1}) was observed in the Raman spectrum, indicating that the structural distortion of the graphite sheet by N-doping occurred and large amounts of topological defects were introduced.[7] As seen in Figure 2, the G band of NG was located at 1582 cm^{-1}. Usually, the G band of pristine graphene appeared at 1585−1588 cm^{-1}.[8] It seems that the position of the G band of the graphite sheet was changed during the synthesis of NG. Typically, there

are many factors influencing the position of the G band, such as doping,[23] layer numbers,[24] and defects.[8] The downshift of the G band in the present study might be related to N-doping, which was also observed by Guo *et al*., who reported that the G band of the Raman spectrum was shifted about 15 cm^{-1} by hetero N atoms during the synthesis of NG.[25] The I_D/I_G (a peak intensity ratio of D to G band) was estimated to be 0.22, which suggested that the NG layer remained at a high crystalline quality. The X-ray diffraction (XRD) profile is shown in Figure S2 (Supporting Information), and a pronounced peak at 26.1° characteristic of nitrogen-free graphene was observed, further evidencing the high quality of the synthesized NG. The background band centered at 26.1° might be attributed to the presence of intercalated "N defeats" in the NG structure. From the diffraction peak positions, the *d*-spacing for NG was calculated to be 3.49 Å, which showed good conformity with the TEM analyses. The 2D band, the most prominent feature in the Raman spectra, was located at 2648 cm^{-1}. In most cases, the shape of the 2D band with a broad peak at 2650 cm^{-1} corresponds to the multilayer graphene.[8] Therefore, the NG prepared in this work was a multilayer graphene, which was also seen in Figure 1C.

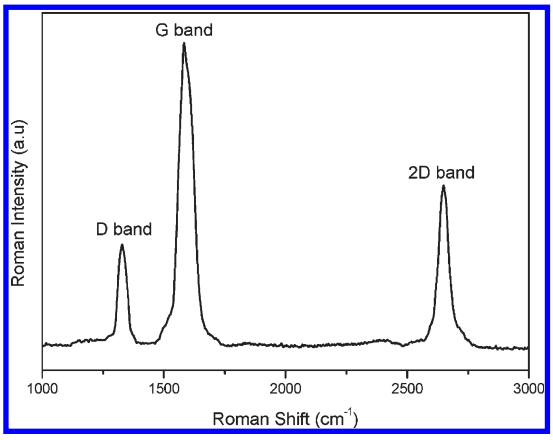

Figure 2. Raman spectrum of the synthesized NG.

XPS is a commonly used technique to examine the features of nitrogen species in carbon materials such as graphite and carbon nanotubes. The XPS spectrum of synthesized NG over a wide range of binding energy (0−900 eV) is illustrated in Figure 3A. The XPS spectrum had a predominant narrow graphitic C 1s peak at 284.8 eV, along with an obvious N 1s peak at 400.1 eV. The atomic ratio of N/C was calculated to be 12.5% from the peak areas of C 1s and N 1s and their atomic sensitivity factors. Generally, the reported atomic ratio of N/C in the N-doped graphene was around 1−4%.[8−10] The carbon nanomaterials with higher atomic ratios of N/C have been reported to exhibit better physical and chemical properties, such as electrical conductivity and electrocatalytic activity for reduction of hydrogen peroxide.[10,26] It can be seen from this study that the detonation technique benefited the atomic ratio of N/C significantly, which might be an important basis for a wider range of practical applications of NG.

The high-resolution XPS N 1s spectrum is shown in the inset of Figure 3A. Typically, the N 1s peak is absent in the pristine graphene. In the spectrum of NG, however, the N 1s peak appeared and had three components, suggesting that the N atoms were in three different bonding characters inserted into the graphene network (Figure 3B). The peak at 398.7 and 400.1 eV corresponded to pyridinic-like and pyrrolic-like nitrogen atoms, respectively. Pyridinic-N is a type of nitrogen that contributes one p-electron to the aromatic π-system and has a lone electron pair in the plane of the carbon matrix, which can increase the electron-donor property of the catalyst.[27] The peak at 401.7 eV reflected the presence of graphitic-N, which refers to N atoms replacing the C atoms inside the graphene layers. It can also been seen in Figure 3A that the peak for graphitic-N was smaller than those of pyridinic-N and pyrrolic-N, implying that pyridinic-N

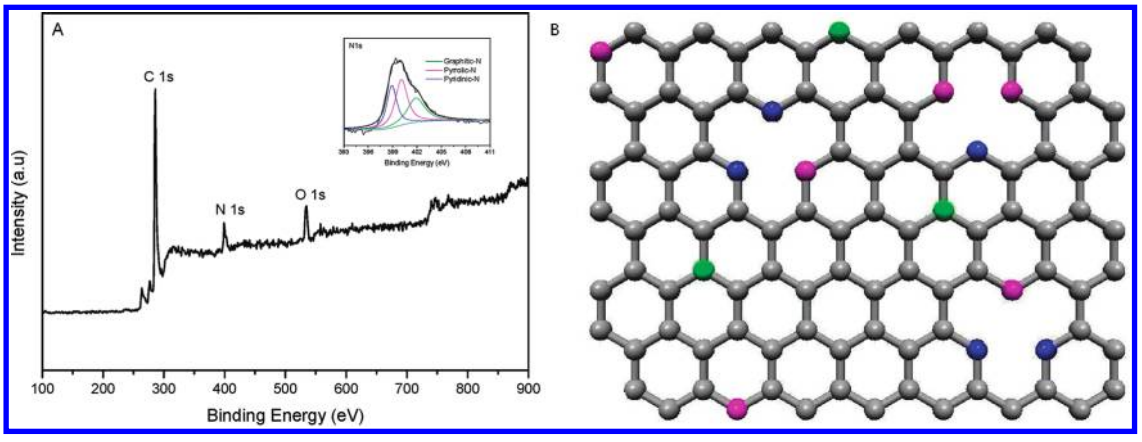

Figure 3. XPS survey of the synthesized NG. Inset shows the high-resolution N 1s spectrum (A). Schematic representation of the N-doped graphene. The gray, green, blue, and magenta spheres represent the C, "graphitic" N, "pyridinic" N, and "pyrrolic" N atoms in the NG, respectively (B).

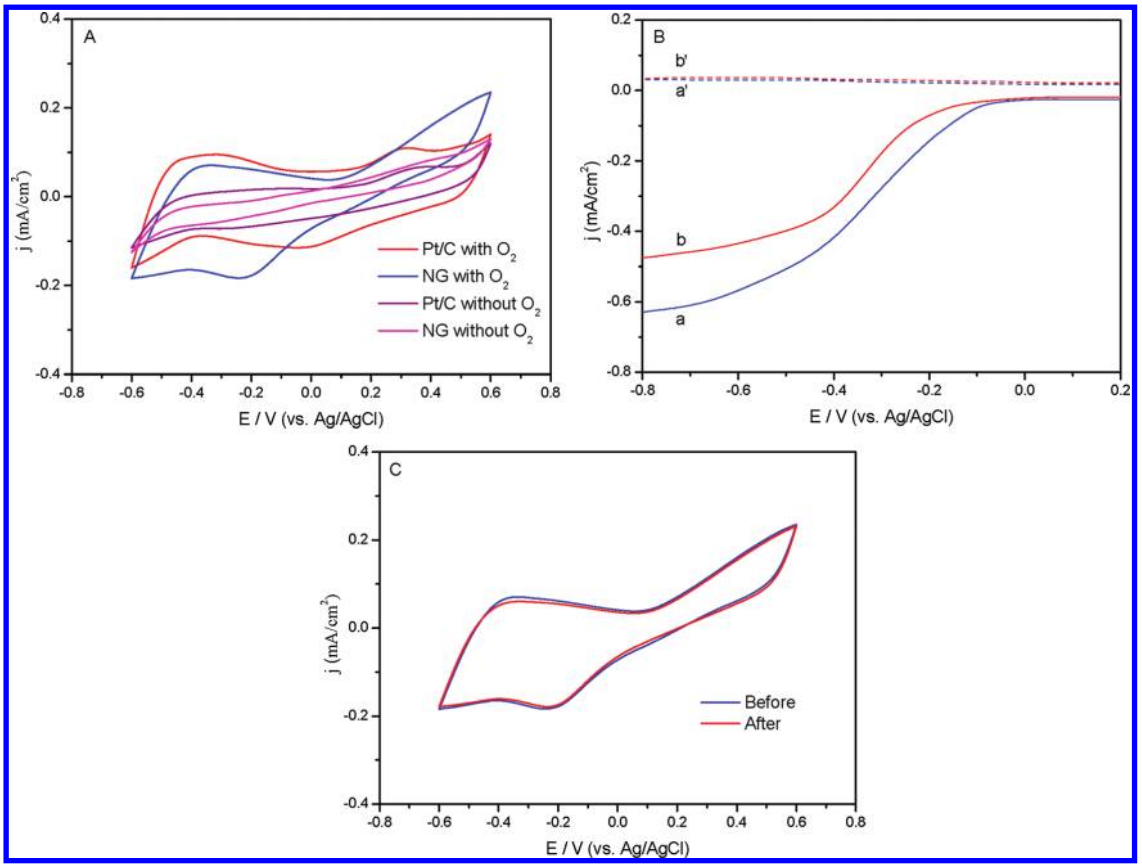

Figure 4. CVs of synthesized NG *versus* commercial Pt/C electrodes in the O_2-saturated/free 50 mM PBS solution (pH 7.0) (A), rotating ring-disk electrode (RRDE) voltammograms of NG (curves a and a′) and Pt/C (curves b and b′) electrodes at a rotation rate of 1200 rpm (B), and CVs of NG electrode before (solid line) and after (dashed line) a continuous potentiodynamic sweep for 100 000 cycles at room temperature (25 °C) (C). The electrolyte used for both RRDE voltammogram and potentiodynamic measurements was an O_2-saturated 50 mM PBS solution (pH 7.0).

and pyrrolic-N dominated in the synthesized NG. In addition to the C 1s and N 1s peaks, an O 1s peak at 536.8 eV was observed for the synthesized NG, possibly due to the incorporation of physically adsorbed oxygen.[28] This obvious O 1s peak might be an additional advantage for the current NG as catalysts of the ORR electrode because it has been reported that graphene with a higher O 1s peak has a stronger ability for O_2 adsorption, which is very important for ORR.[7] Also, it should be emphasized that in the XPS spectrum no metal peaks appeared besides those of C, N, and O, suggesting that the NG was completely metal-free. During the growth of NG in this study, unlike those previously prepared by using metal catalysts, no such metal materials were used, which was the reason that the synthesized NG was metal-free.

In the literature, nitrogen-doped graphene has been demonstrated to display a high electrocatalytic activity for ORR in alkaline solution.[7] To understand the electrocatalytic activity of synthesized NG for ORR in neutral pH media, which are commonly applied as the electrolyte in biological systems, the cyclic voltammetry (CV) measurement was conducted for a glassy carbon (GC) electrode coated with NG (NG/GC) in O_2-saturated/free 50 mM PBS (pH 7.0), while that for GC with a commercial Pt catalyst (20% of Pt/C, BASF) (Pt/C/GC) was set as the control. As shown in Figure 4A, both Pt/C/GC and NG/GC in the presence of oxygen exhibited a clear ORR peak in neutral PBS. When the electrodes were scanned in the absence of oxygen, however, no ORR peak was acquired. The comparison of the ORR CVs of NG/GC and Pt/C/GC revealed that they had similar positions, shapes, and intensities. This similarity unambiguously demonstrated that the NG synthesized by the denotation technique in the current study possessed an excellent electrocatalytic activity for ORR in neutral PBS.

It is well known that ORR is a rather complex multistep process, and the electrocatalytic performance of the cathode catalyst depends on the route of ORR. In this study the RRDE voltammograms were performed to further investigate the electrocatalytic activities and routes of NG and Pt/C for ORR under the steady-state conditions in neutral PBS. It was observed in Figure 4B that the one-step and four-electron pathway for ORR occurred at Pt/C/GC. Similar to Pt/C/GC, NG/GC also exhibited a one-step process for ORR at the onset potential of about −0.04 V, which was confirmed by the nearly negligible corresponding current for HO_2^- oxidation recorded at the Pt ring electrode (a′, blue

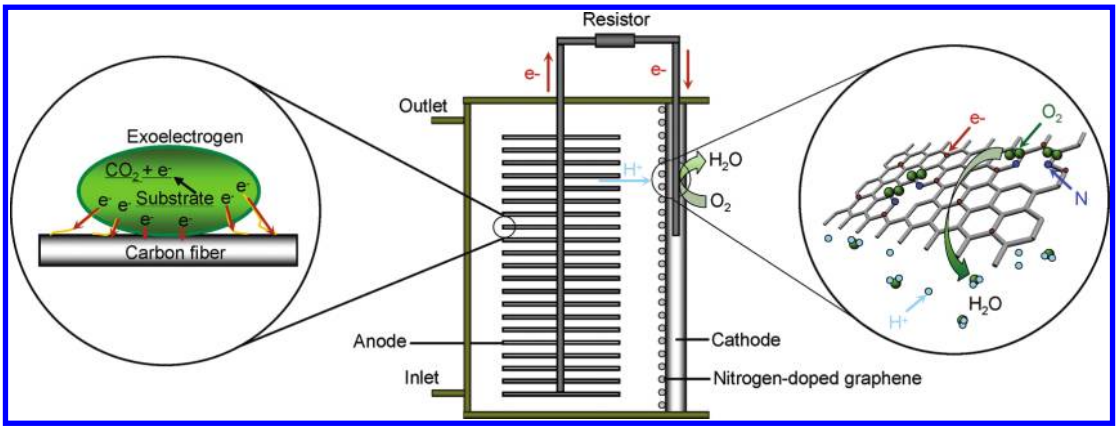

Figure 5. Schematic of a membrane-free single-chamber air-cathode MFC showing the basic mechanism of current generation.

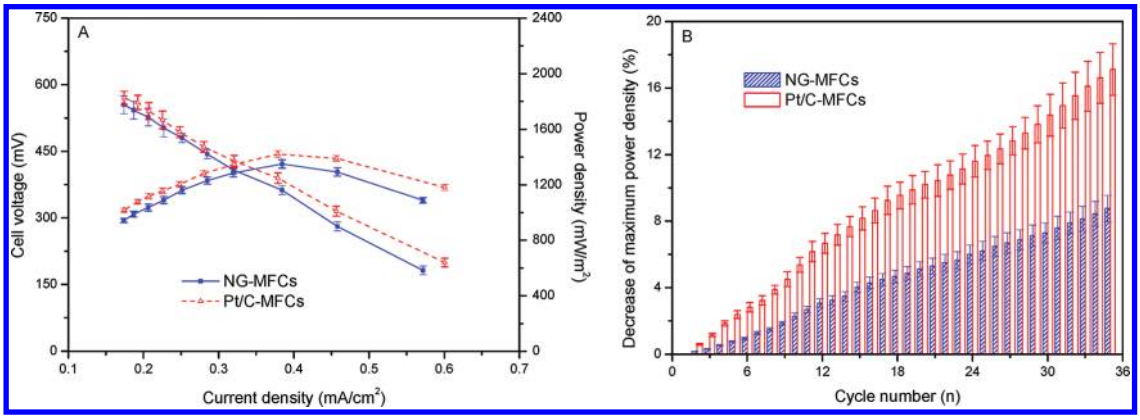

Figure 6. Power densities and cell voltages in NG-MFCs and Pt/C-MFCs (A). Decrease of the maximum power density as a function of cycle number at an external resistance of 1000 Ω. 35 cycles represent about 70 days (B). Error bars represent standard deviations of duplicate tests.

dashed line). The transferred electron number ($n = 4I_D/(I_D + I_R/N)$, where I_D is the faradic disk current, I_R is the faradic ring current, and $N = 0.47$ is the collection efficiency determined with $Fe(CN)_6^{3-/4-}$ as probe) per oxygen molecule involved in the oxygen reduction was calculated to be 3.69 for NG/GC at the potential of −0.40 V, indicating that the reduction process of NG was a combination of two-electron and four-electron pathways. The above voltammetry measurements demonstrated that the NG synthesized in this study had an outstanding electrocatalytic activity for ORR in the neutral PBS solution.

The stability is always a key feature of catalysts when being used to catalyze the ORR in aqueous solution. In order to get insight into the electrocatalytic stability of NG, the voltammetry experiments were carried out by cycling the potential between −0.8 and 0.8 V in O_2-saturated 50 mM neutral PBS before and after a continuous potentiodynamic sweep. As can be seen in Figure 4C, almost no significant loss in the electrochemical activity was observed after 100 000 continuous cycles, suggesting that the elctrocatalytic stability of NG for oxygen reduction was excellent in the neutral PBS solution. Also investigated in this study was the crossover behavior of synthesized NG in the PBS solution with 5 mM Na-formate (Figure S3 in the Supporting Information). It is clearly visible that the ORR performance at the NG electrode remained largely unaffected in the presence of formate (a common microbial metabolite), which might be another advantage of the NG used as ORR catalyst in biological systems.

As oxygen is the most sustainable electron acceptor at the cathode of MFCs and the synthesized NG has been demonstrated to possess an excellent electrocatalytic activity for ORR in neutral PBS, the performance of MFCs with NG as the cathode catalyst (shortened as NG-MFCs, Figure 5) in batch mode was examined using acetate synthetic wastewater as the fuel, and MFCs with Pt/C (Pt/C-MFCs) were set as the contrast. The obtained polarization curves and power densities are presented in Figure 6A. It can be seen that the voltage generated in NG-MFCs was 0.555 ± 0.025 V at an external resistance of 1000 Ω, close to that in Pt/C-MFCs (0.570 ± 0.015 V). Also as seen in Figure 6A, the NG-MFCs produced a maximum power density of 1350 ± 15 mW/m^2, which was much close to that generated by Pt/C-MFCs (1420 ± 25 mW/m^2). The power output in

NG-MFCs was competitive, which was just slightly less (5%) than that in Pt/C-MFCs. In the literature, many efforts have been made to develop alternative catalysts, such as activated carbon,[29] graphite,[30] enzymes,[31] microorganism,[32] transition metal porphyrines, and phthalocyanines,[33−36] to replace or reduce Pt in MFCs due to its high cost. As far as we know, however, when those cathode catalysts were used, the power output was much lower than that with Pt/C.

In this study the internal resistances of NG-MFCs and Pt/C-MFCs, based on EIS analysis, were determined to be 98 ± 2 and 85 ± 3 Ω, respectively. As is well known, the internal resistance of a MFC consists of two parts: the electrolyte ohmic loss due to the movement of electrons through the electrolyte, and the electrode ohmic loss caused by the movement of electrons through the electrode and wires. Here, two kinds of MFC reactors (NG-MFCs and Pt/C-MFCs) had the same configuration, such as anode material and electrode distance. The difference in internal resistance between NG-MFCs and Pt/C-MFCs therefore came from the diversity of the electrical characteristics, especially the conductivity, between the synthesized NG and Pt/C. The measured electrical conductivities of NG and Pt/C cathodes were 35 ± 3 and 45 ± 5 S/cm, respectively. Clearly, the lower conductivity of the NG cathode, compared with that of the Pt/C cathode, led to a higher internal resistance of NG-MFCs. Although the internal resistance of MFCs was slightly higher, the power output in NG-MFCs was still analogous to that in Pt/C-MFCs, suggesting that the synthesized NG had a great potential to be used as an alternative to Pt/C in MFCs.

In order to investigate the stability of the synthesized NG in MFCs, the decrease of maximum power density with cycle number (*i.e.*, operation time) was examined. It can be seen from Figure 6B that after 35 operation cycles (~70 d) the decrease of maximum power density in NG-MFCs was 8.8 ± 0.8%, whereas it was 17.1 ± 0.6% in Pt/C-MFCs. Obviously, NG-MFCs produced electricity more stably than Pt/C-MFCs. It has been proposed that the decline of maximum power density over operation time in Pt/C-MFCs was due to the proton limitation caused by biofilm formation on the cathode surface and the deterioration of electrocatalytic activity of the cathode catalyst.[34] In this study the thickness of biofilms on the cathodes of NG-MFCs and Pt/C- MFCs was about 0.1 cm after 35 operation cycles, which might be one of the reasons for the decrease of maximum power density. However, it is noted that the loss of power density in MFCs without cathode catalyst, which was caused by proton limitation only, was 1.1 ± 0.1% (detailed data not shown in Figure 6B), indicating that the deterioration of electrocatalytic activity of cathode catalyst was the main reason for the drop of maximum power density in NG-MFCs and Pt/C-MFCs. The synthesized NG catalyst had superb electrocatalytic stability for ORR and could be used as a promising catalyst in MFCs with a long run.

As mentioned above, the practical applications of MFCs are largely limited by the high cost of the cathode catalyst, especially as the scale increases. The prices of cyanuric chloride and trinitrophenol at present are $0.07 and $0.12 per gram, respectively, and the reagent cost of per gram NG in this study was approximately $2.5 ((0.07 + 0.12 × 3 ÷ 2) × 1 ÷ 0.1 = 2.5). Normally, the conventional Pt/C is prepared with Pt salts, such as dihydrogen hexachloroplatinate(IV) hexahydrate, and carbon supports by complex techniques with impregnation and reduction.[37] Nowadays, the price of dihydrogen hexachloroplatinate(IV) hexahydrate with a Pt content of 37.5% is about $122.9/g, and the reagent cost for Pt/C containing 1 g of Pt is therefore $327.7 (122.9 ÷ 37.5% = 327.7) when only the cost of Pt salt was considered. Clearly, the reagent cost for NG synthesis in the current work was much lower than that of Pt/C. Considering the complex process for the synthesis of Pt/C, it can be anticipated that the NG synthesized in this study would be much less expensive than the conventional Pt/C, and the power per cost in NG-MFCs would also be much greater than that in Pt/C-MFCs.

CONCLUSIONS

In this study, we provided a simple approach to prepare NG at low temperature using a denotation process with cyanuric chloride and trinitrophenol as reagents, and a gram scale was easily obtained in the laboratory. This method allowed scalable synthesis, standing as a complementary route for large-scale growth of NG. By using TEM, Raman, XRD, and XPS, we demonstrated that nitrogen species were incorporated into the graphene structure with a high atomic ratio of N/C, and the synthesized NG was high-quality multilayered graphene. Also, the NG showed an excellent electrocatalytic activity and stability for ORR in neutral PBS and was applied successfully as an efficient metal-free and less expensive cathode catalyst of MFCs compared with Pt catalyst. This novel cathode catalyst, as an alternative to Pt/C, might offer a new potential for constructing a high-performance and less expensive cathode, which is crucial for the large-scale application of MFCs.

EXPERIMENTAL SECTION

NG Preparation. NG was synthesized with the detonation technique. Unless otherwise stated, all chemicals were purchased from Alfa Aesar (99.99% purity) and used without any further purification. All the solutions were prepared with doubly distilled water.

Material and Electrochemical Analyses. Transmission electron microscopy (TEM) images for NG were recorded on a Philips EM-430 TEM unit. Raman microspectroscopy was carried out on a Renishaw inVia unit using an Ar ion laser with an excitation wavelength of 514.5 nm. The wide-angle X-ray diffraction pattern was recorded on a Bruker D8 Advance X-ray diffractometer with Cu Kα radiation. The diffraction data were collected in step scans, with a step size of 0.05° (2θ) and a count time of 2 s per step between 10° and 100° (2θ). X-ray photoelectron spectroscopic measurements were performed on a Perkin-Elmer PHI 5000C ESCA system using a monochromic Al Kα X-ray source.

Electrochemical measurements were conducted on a computer-controlled electrochemical workstation (CHI 760C, CH Instrument, USA) with a typical three-electrode cell equipped with gas flow systems. NG/GC or Pt/C/GC was used as working electrode, an Ag/AgCl electrode (3 M KCl-filled) as reference electrode, and a platinum wire as counter electrode. An aqueous solution of 50 mM PBS (pH 7.0) was applied as the electrolyte for both CV and RRDE voltammogram measurements. CV was used to characterize the electrochemical activities on the electrode surface by measuring the current response at an electrode surface to a specific range of potentials with a scan rate of 0.1 V/s. The RRDE experiments were also carried out on the CHI 760C workstation with a rotation speed controller (Pine Research Instrument Co., USA). The potential was varied from 0.4 to −0.8 V *vs* Ag/AgCl at a potential sweep rate of 0.01 V/s. The ink for RRDE consisted of 2 mg of catalyst (NG or Pt/C) suspended in 2 mL of 0.2 wt % Nafion solution. Before the RRDE experiments, 20 μL of catalyst ink was coated onto the glassy carbon electrode, and oxygen gas was saturated in the electrolyte by bubbling the gas for 30 min. All electrochemical experiments (except as noted) were carried out at room temperature (25 ± 1 °C).

The internal resistance (R_{in}) of MFCs was determined by electrochemical impedance spectroscopy (EIS) according to the method of Bard *et al.*[38] Impedance measurements were conducted at open circuit voltage over a frequency range of 0.05 to 10^5 Hz with a sinusoidal perturbation amplitude of 10 mV. After the MFCs generated power stably, the external resistance (R_{ext}) was in turn shifted in the range of 10 to 10^4 Ω to prepare the polarization and power curves. At each resistance, MFCs were operated for at least two batches to ensure a repeatable voltage output. The electrical conductivities of NG and Pt/C used in this study were determined at 25 ± 1 °C according to the method of Park *et al.*[39] The concentration of acetate in MFCs was determined on the basis of the method described in our previous study.[40] All samples were filtered through a Whatmann GF/C glass microfiber (pore size 0.45 μm) before measurements.

MFC Setup and Operation. The membrane-free single-chamber air−cathode MFCs consisted of a carbon fiber brush anode and carbon cloth cathode as previously reported.[41] When being applied as the cathode catalyst, NG, with a loading of 0.5 mg/cm^2, was coated on the water-facing side using a binder of Nafion and isopropyl alcohol, with four PTFE diffusion layers and one carbon base layer on the air-facing side. In order to compare the performance of NG with the commonly used cathode catalyst, MFCs with Pt/C were examined as the comparison. Also, MFCs containing only carbon powder (Vulcan XC-72) on the cathode were set as the noncatalyst control to investigate the elctrocatalytic stability of cathode catalysts.

MFCs (duplicate reactors), inoculated with suspended bacteria from an acetate-fed MFC reactor that had been operating for about 5 months, were filled with acetate-laden synthetic wastewater containing (1 L of 50 mM phosphate buffer solution, pH 7.0) NaAc (a preferred carbon source for exoelectrogenic bacteria[16]), 1000 mg; NH_4Cl, 310 mg; KCl, 130 mg; and a mineral (12.5 mL) and vitamin (12.5 mL) as described by Lovely and Phillips.[42] The feed solution was replaced when the voltage dropped below 20 mV, forming one complete cycle of operation. The inoculum was omitted from the solution when stable voltages were produced after inoculation for approximately 500 h. The external resistance was fixed at 1000 Ω (except as noted), and all reactors were operated in batch mode at room temperature (25 ± 1 °C).

Calculations. Voltage yield from MFCs was recorded with a multicoated voltage collection instrument (12-bit A/D-conversion chips, USA) connected to a personal computer *via* a universal serial bus (USB) (Intel, USA) interface and calibrated with a digital multimeter (Fluke 15B; Fluke, USA) before each test. Power density was calculated according to P (mW/m^2) = $10E^2/(R_{ext}A)$, where the factor of 10 is needed for the given units, E (mV) is the voltage, R_{ext} (Ω) is the external resistance, and A (cm^2) is the project surface area of the electrode in MFCs.

Acknowledgment. This work was financially supported by the Foundation of State Key Laboratory of Pollution Control and Resources Reuse (Tongji University) (Nos. PCRRK and PCRRY 10001), Fundamental Research Funds for the Central Universities, and China Postdoctoral Science Foundation (Nos. 20100470730 and 201104283).

Supporting Information Available: This file contains Figures S1−S3. This material is available free of charge *via* the Internet at http://pubs.acs.org.

REFERENCES AND NOTES

1. Liu, C. G.; Yu, Z. N.; Neff, D.; Zhamu, A.; Jang, B. Z. Graphene-Based Supercapacitor with an Ultrahigh Energy Density. *Nano Lett.* **2010**, *10*, 4863–4868.
2. Wang, Y.; Yang, R.; Shi, Z. W.; Zhang, L. C.; Shi, D. X.; Wang, E. G.; Zhang, G. Y. Super-Elastic Graphene Ripples for Flexible Strain Sensors. *ACS Nano* **2011**, *5*, 3645–3650.
3. Subrahmanyam, K. S.; Kumar, P.; Maitra, U.; Govindaraj, A.; Hembram, K. P. S. S.; Waghmare, U. V.; Rao, C. N. R. Chemical Storage of Hydrogen in Few-Layer Graphene. *Proc. Natl. Acad. Sci. U. S. A.* **2011**, *108*, 2674–2677.
4. Li, Y. F.; Zhou, Z.; Shen, P. W.; Chen, Z. F. Spin Gapless Semiconductor−Metal−Half-Metal Properties in Nitrogen-Doped Zigzag Graphene Nanoribbons. *ACS Nano* **2009**, *3*, 1952–1958.
5. Yu, S. S.; Zheng, W. T.; Wang, C.; Jiang, Q. Nitrogen/Boron Doping Position Dependence of the Electronic Properties of a Triangular Graphene. *ACS Nano* **2010**, *4*, 7619–7629.
6. Li, X. L.; Wang, H. L.; Robinson, J. T.; Sanchez, H.; Diankov, G.; Dai, H. J. Simultaneous Nitrogen Doping and Reduction of Graphene Oxide. *J. Am. Chem. Soc.* **2009**, *131*, 15939–15944.
7. Qu, L. T.; Liu, Y.; Baek, J.; Dai, L. M. Nitrogen-Doped Graphene as Efficient Metal-Free Electrocatalyst for Oxygen Reduction in Fuel Cells. *ACS Nano* **2010**, *4*, 1321–1326.
8. Wei, D. C.; Liu, Y. Q.; Wang, Y.; Zhang, H. L.; Huang, L. P.; Yu, G. Synthesis of N-Doped Graphene by Chemical Vapor Deposition and Its Electrical Properties. *Nano Lett.* **2009**, *9*, 1752–1758.
9. Reddy, A. L. M.; Srivastava, A.; Gowda, S. R.; Gullapalli, H.; Dubey, M.; Ajayan, P. M. Synthesis of Nitrogen-Doped Graphene Films for Lithium Battery Application. *ACS Nano* **2010**, *4*, 6337–6342.
10. Panchakarla, L. S.; Subrahmanyam, K. S.; Saha, S. K.; Govindaraj, A.; Krishnamurthy, H. R.; Waghmare, U. V.; Rao, C. N. R. Synthesis, Structure, and Properties of Boron- and Nitrogen-Doped Graphene. *Adv. Mater.* **2009**, *21*, 4726–4730.
11. Wang, X. R.; Li, X. L.; Zhang, L.; Yoon, Y.; Weber, P. K.; Wang, H. L.; Guo, J.; Dai, H. J. N-Doping of Graphene Through Electrothermal Reactions with Ammonia. *Science* **2009**, *324*, 768–771.
12. Jin, Z.; Yao, J.; Kittrell, C.; Tour, J. M. Large-Scale Growth and Characterizations of Nitrogen-Doped Monolayer Graphene Sheets. *ACS Nano* **2011**, *5*, 4112–4117.
13. Tang, Y.; Allen, B. L.; Kauffman, D. R.; Star, A. Electrocatalytic Activity of Nitrogen-Doped Carbon Nanotube Cups. *J. Am. Chem. Soc.* **2009**, *131*, 13200–13201.
14. Logan, B. E. Exoelectrogenic Bacteria that Power Microbial Fuel Cells. *Nat. Rev. Microbiol.* **2009**, *7*, 375–381.
15. Xie, X.; Hu, L. B.; Pasta, M.; Wells, G. F.; Kong, D. S.; Criddle, C. S.; Cui, Y. Three-Dimensional Carbon Nanotube-Textile Anode for High-Performance Microbial Fuel Cells. *Nano Lett.* **2011**, *11*, 291–296.

16. Logan, B. E.; Regan, J. M. Microbial Fuel Cells Challenges and Applications. *Environ. Sci. Technol.* **2006**, *40*, 5172–5180.
17. Zhao, F.; Harnisch, F.; Schröder, U.; Scholz, F.; Bogdanoff, P.; Herrmann, I. Challenges and Constraints of Using Oxygen Cathodes in Microbial Fuel Cells. *Environ. Sci. Technol.* **2006**, *40*, 5193–5199.
18. Liu, H.; Ramnarayanan, R.; Logan, B. E. Production of Electricity during Wastewater Treatment Using a Single Chamber Microbial Fuel Cell. *Environ. Sci. Technol.* **2004**, *38*, 2281–2285.
19. Tender, L. M.; Reimers, C. E.; Stecher, H. A., III; Holmes, D. E.; Bond, D. R.; Lowy, D. A.; Pilobello, K.; Fertig, S. J.; Lovley, D. R. Harnessing Microbially Generated Power on the Seafloor. *Nat. Biotechnol.* **2002**, *20*, 821.
20. Zuo, Y.; Maness, P.; Logan, B. E. Electricity Production from Steam-Exploded Corn Stover Biomass. *Energy Fuels* **2006**, *20*, 1716–1721.
21. Geim, A. K.; Novoselov, K. S. The Rise of Graphene. *Nat. Mater.* **2007**, *6*, 183–191.
22. Meyer, J. C.; Geim, A. K.; Katsnelson, M. I.; Novoselov, K. S.; Booth, T. J.; Roth, S. The Structure of Suspended Graphene Sheets. *Nature* **2007**, *446*, 60–63.
23. Pisana, S; Lazzeri, M.; Casiraghi, C.; Novoselov, K. S.; Geim, A. K.; Ferrari, A. C.; Mauri, F. Breakdown of the Adiabatic Born-Oppenheimer Approximation in Graphene. *Nat. Mater.* **2007**, *6*, 198–201.
24. Graf, D.; Molitor, F.; Ensslin, K.; Stampfer, C.; Jungen, A.; Hierold, C.; Wirtz, L. Spatially Resolved Raman Spectroscopy of Single- and Few-Layer Graphene. *Nano Lett.* **2007**, *7*, 238–242.
25. Guo, B. D.; Liu, Q.; Chen, E. D.; Zhu, H. W.; Fang, L.; Gong, J . R. Controllable N-Doping of Graphene. *Nano Lett.* **2010**, *10*, 4975–4980.
26. Wang, Y.; Shao, Y. Y.; Matson, D. W.; Li, J. H.; Lin, Y. H. Nitrogen-Doped Graphene and Its Application in Electrochemical Biosensing. *ACS Nano* **2010**, *4*, 1790–1798.
27. Liu, G.; Li, X. G.; Popov, B. N. Development of Non-Precious Oxygen Reduction Catalysts from N-Doped Ordered Porous Carbon. *Appl. Catal. B: Environ.* **2009**, *93*, 156–165.
28. Collins, P. G.; Bradley, B.; Ishigami, M.; Zettl, A. Extreme Oxygen Sensitivity of Electronic Properties of Carbon Nanotubes. *Science* **2000**, *287*, 1801–1804.
29. Deng, Q.; Li, X. Y.; Zuo, J. E.; Logan, B. E. Power Generation Using an Activated Carbon Fiber Felt Cathode in an Upflow Microbial Fuel Cell. *J. Power Sources* **2010**, *195*, 1130–1135.
30. Tran, H. T.; Ryu, J. H.; Jia, Y. H.; Oh, S. J.; Choi, J. Y.; Park, D. H.; Ahn, D. H. Continuous Bioelectricity Production and Sustainable Wastewater Treatment in a Microbial Fuel Cell Constructed with Non-Catalyzed Granular Graphite Electrodes and Permeable membrane. *Water Sci. Technol.* **2010**, *61*, 1819–1827.
31. Schaetzle, O.; Barrière, F.; Schröder, U. An Improved Microbial Fuel Cell with Laccase as the Oxygen Reduction Catalyst. *Energy Environ. Sci.* **2009**, *2*, 96–99.
32. Cao, X. X.; Huang, X.; Liang, P.; Boon, N.; Fan, M. Z.; Zhang, L.; Zhang, X. Y. A Completely Anoxic Microbial Fuel Cell Using a Photo-Biocathode for Cathodic Carbon Dioxide Reduction. *Energy Environ. Sci.* **2009**, *2*, 498–501.
33. Qiao, Y.; Bao, S. J.; Li, C. M. Electrocatalysis in Microbial Fuel Cells—from Electrode Material to Direct Electrochemistry. *Energy Environ. Sci.* **2010**, *3*, 544–553.
34. Cheng, S. A.; Liu, H.; Logan, B. E. Power Densities Using Different Cathode Catalysts (Pt and CoTMPP) and Polymer Binders (Nafion and PTFE) in Single Chamber Microbial Fuel Cells. *Environ. Sci. Technol.* **2006**, *40*, 364–369.
35. Yu, E. H.; Cheng, S. A.; Scott, K.; Logan, B. E. Microbial Fuel Cell Performance with Non-Pt Cathode Catalysts. *J. Power Sources* **2007**, *171*, 275–281.
36. Zhang, L. X.; Liu, C. S.; Zhuang, L.; Li, W. S.; Zhou, S. G.; Zhang, J. T. Manganese Dioxide as an Alternative Cathodic Catalyst to Platinum in Microbial Fuel Cells. *Biosens. Bioelectron.* **2009**, *24*, 2825–2829.
37. Xue, B.; Chen, P.; Hong, Q.; Li, J. Y.; Tan, K. L. Growth of Pd, Pt, Ag and Au Nanoparticles on Carbon Nanotubes. *J. Mater. Chem.* **2001**, *11*, 2378–2381.
38. Bard, A. J.; Faulkner, L. R. *Electrochemical Methods: Fundamentals and Applications*, 2nd ed.; John Wiley & Sons: New York, 2001.
39. Park, Y. T.; Ham, A. Y.; Grunlan, J. C. High Electrical Conductivity and Transparency in Deoxycholate-Stabilized Carbon Nanotube Thin Films. *J. Phys. Chem. C* **2010**, *114*, 6325–6333.
40. Feng, L. Y.; Chen, Y. G.; Zheng, X. Enhancement of Waste Activated Sludge Protein Conversion and Volatile Fatty Acids Accumulation during Waste Activated Sludge Anaerobic Fermentation by Carbohydrate Substrate Addition: The Effect of pH. *Environ. Sci. Technol.* **2009**, *43*, 4373–4380.
41. Feng, L. Y.; Yan, Y. Y.; Chen, Y. G.; Wang, L. J. Nitrogen-Doped Carbon Nanotubes as Efficient and Durable Metal-Free Cathodic Catalyst for Oxygen Reduction in Microbial Fuel Cells. *Energy Environ. Sci.* **2011**, *4*, 1892–1899.
42. Lovley, D. R.; Phillips, E. J. P. Novel Mode of Microbial Energy Metabolism: Organic Carbon Oxidation Coupled to Dissimilatory Reduction of Iron or Manganese. *Appl. Environ. Microbiol.* **1988**, *54*, 1472–1480.